16th International Conference on

Computer and IT Applications in the Maritime Industries

COMPIT'17

Cardiff, 15-17 May 2017

Edited by Volker Bertram

TUHH
Technische Universität Hamburg-Harburg
Institut für Entwerfen von Schiffen und Schiffsicherheit
Schwarzenbergstraße 95 Gebäude C D-21073 Hamburg

TuTech
TUHH Technologie GmbH

16th International Conference on Computer and IT Applications in the Maritime Industries, Cardiff, 15-17 May 2017**,** Hamburg, Technische Universität Hamburg-Harburg, 2017, ISBN 978-3-89220-701-6

Schriftenreihe Schiffbau
Schwarzenbergstraße 95c
D-21073 Hamburg
http://www.tuhh.de/vss

Index

Sea Currents and Waves for Optimal Route Planning with VISIR

Gianandrea Mannarini, Giovanni Coppini, Rita Lecci, Giuseppe Turrisi,
Fondazione CMCC, Lecce/Italy, gianandrea.mannarini@cmcc.it

Abstract

The open-source model for marine-weather ship routing VISIR (visir-model.net) was designed in a modular way for easily modifying and adding functionalities. In particular, the impact of ocean currents is the subject of the latest development. The model has been extended for using forecasts of surface sea currents from the European service CMEMS (marine.copernicus.eu). However, fields from other providers can be easily used. Currents are shown to have an impact in the percent range on route duration - even in presence of waves - and can also affect route topology in specific cases, demonstrating that even short-sea shipping could benefit from accounting for forecast ocean state.

1. Introduction

Meteo-oceanographic forecasts may be exploited for optimising navigation between given end-points with respect to some strategic objective such as route duration or fuel oil consumption. The International Maritime Organization recommends to avoid "rough seas and head currents" among the ten measures within the Ship Energy Efficiency Management Plan (SEEMP), *Bazari and Longva (2011)*. The SEEMP is one of the main instruments for the mitigation of the contribution of maritime transportation to climate change, *Mannarini (2015a)*.

A reconstruction of the Kuroshio current by means of drifter data is employed by *Chang et al. (2013)* for demonstrating that it can be exploited for time-savings when navigating between Taipei and Tokyo (about 1100 *M* distance (1 M = 1850 m)). In that work, suggested diversions from the great circle route are seemingly ad hoc chosen, without any automatic optimisation procedure. Nevertheless, the authors find that the proposed route, despite extra mileage, leads to savings in the 2-6% range for super-slow-steaming (12 kn) vessels. The largest savings are obtained for the south-west-bound route (against the Kuroshio).

Lo and McCord (1995) report significant fuel savings in the Gulf Stream region (up to 6-9%) for routes with or against the main current direction. Per construction, routes of constant duration and constant speed through water (STW) were considered. The horizontal spacing of the current fields employed varied from 5 to 0.1 degree, with best performances in fuel savings at the highest spatial resolution. The same authors also developed an algorithm that tackles the problem of the predictability of ocean currents, especially where they are stronger and thus more dynamic, *Lo and McCord (1998)*. Their approach is based on a stochastic variant of the dynamic programming technique by *Chen (1978)* or *Zoppoli (1972)*. As such, there are inherent simplifications of the route geometry, e.g. it cannot sail trough the same longitude on more than a single waypoint (WP) and it is unclear how to deal with coastline and other topological restrictions.

An exact method based on the level set equation has been developed by *Lolla et al. (2014)* and it can deal with generic time-dependent flows and vehicle speeds through the flow. It is based on two-step differential equations governing the propagation of the reachability front (a Hamilton-Jacobi level-set equation) and the time-optimal trajectory (a particle backnracking ordinary differential equation). The paper by *Lolla et al. (2014)* contains a careful analysis of the mathematical scheme and the computational cost. The level set approach was extended to deal with energy minimisation by *Subramani et al. (2016)* showing the potential of intentional speed reduction in a dynamic flow. This method appears to be quite promising, though is not yet employed in an operational environment.

The above recognition of literature shows that the question of the impact of sea/ocean currents on navigation, despite its classical appearance, is still open. In fact, the available results are hardly

comparable to each other, since they employ different methods in different regions of the global ocean. Also, none of the cited works considers the impact of ocean currents and waves altogether. Finally, the published methods are just applied to case studies and are not operational.

The latest development of the VISIR model *Mannarini et al. (2016a,b,c)* would like to contribute to these issues. The VISIR model is at the heart of an operational marine-weather routing system for the Mediterranean Sea, www.visir-nav.com. It has been applied also to sailboat routing in *Mannarini et al. (2015b)*. Its algorithm for computing the shortest routes has been validated versus analytical results in case of static wave fields. VISIR is coded in MATLAB and its first version was released with a GPL licence, www.visir-model.net.

2. Model structure

The VISIR model was documented in highest detail in *Mannarini et al. (2016b)*. The inclusion of ocean currents required a few developments that are summarized in this section.

2.1. Speed over ground

Assuming that the vessel speed over ground (SOG) is given by the linear superposition of surface ocean current and vessel speed through water (STW, see Sect.2.2), the rudder can be employed to instantaneously adjust vessel heading for compensating the cross current.

A formal definition of the above statement allows inferring following general features:

a) The cross flow always reduces the SOG, as part of vessel momentum has to be spent for compensating the drift. The flow component along the route instead may either increase or decrease the SOG;
b) The ratio of the cross flow to the magnitude of the STW determines the rudder angle.

The SOG resulting from a) is then used by the VISIR routine for path optimization, as explained in Sect.2.3.

2.2. Speed through water

The STW is defined as the SOG in the absence of ocean currents. Following *Mannarini et al. (2016b)*, the STW is determined by the sea state only. In particular, the STW results from a balance of thrust and resistance at the propeller. In the resistance, a term related to calm water is distinguished from a "wave added resistance". The calm water term depends on a dimensionless drag coefficient C_T that, within VISIR, has a power-law dependence on STW: $C_T \sim (STW)^q$. For the wave added resistance, its directional and spectral dependence is neglected, and just the peak value of the radiation part is considered. The latter is obtained by *Alexandersson (2009)* as a function of vessel's principal particulars, starting from a statistical reanalysis of simulations based on *Gerritsma and Beukelman (1972)*'s method.

Finally, VISIR employs sea-state information also for performing a few checks of vessel intact stability, namely related to: parametric roll, pure loss of stability, and surfriding/broaching-to. The algorithm then constructs the optimal route by ensuring that vessel intact stability is always satisfied.

2.3. Discretisation and graph-search method

The SOG obtained using both ocean currents (Sect.2.1) and the STW depending on sea state (Sect.2.2) are the key ingredients for the computation of the optimal routes. These routes result from a shortest path algorithm on a graph, whose edge weights are given by the rate between the distance between couples of graph nodes and the SOG. Since the SOG depends on time-dependent environmental fields (Sect.2.4), the edge weights too are functions of time. Thus, a classical shortest

path algorithm (Dijkstra's one, cf. *Bertsekas (1998)*) is adapted to time-dependent edge weights in *Mannarini et al. (2016b)*.

Furthermore, several variants of the edge weights are computed, each corresponding to a different value of the vessel's engine throttle. The algorithm then selects the highest throttle leading to a vessel speed that is still compliant with the stability constraints (Sect.2.2). This way, an option of voluntary speed reduction is implemented into the algorithm.

Table I: Connectivity parameters for graphs with squared meshes

Order of neighbours	Min resolution	Max resolution
2	26.6°	18.4°
4	14.0°	4.4°

In the VISIR version described in *Mannarini et al. (2016b)*, a graph mesh with a 1/60 degree spacing (i.e., about 1 M in the meridional direction) and an angular resolution of about 27° were considered. Angular resolution affects route smoothness and, thus, route accuracy and duration. This is especially true in presence of ocean currents, since they form eddies with a radius of curvature about one of order of magnitude smaller than the typical extension of rough seas areas, www.sea-conditions.com, Fig.3. For this reason, the angular resolution of VISIR was improved by considering edges between all nodes up to the fourth and not just the second order of neighbors of a squared mesh. As reported in Table I, this implies that the angular resolution is now between about 14 and 5°, depending on direction.

2.4. Forecasts fields

The developments of VISIR require hydrodynamic and sea-state forecast fields in input. They are both obtained from the CMEMS operational system, marine.copernicus.eu. However, fields from other providers can also be used, just adapting the VISIR functions for field reading.

2.4.1. Surface currents

Forecast fields of surface ocean currents are employed. They are produced by an operational implementation of the hydrodynamic forecasting model NEMO in the Mediterranean Sea, *Tonani et al. (2014,2015)*. The Cartesian components of the current field are horizontally discretized on a 1/16 degree (3.75 M in the meridional direction) mesh and the time-resolution of the output is hourly.

2.4.2. Waves

Forecast fields of significant wave height, wave direction, and mean wave period are employed. They are produced by an operational implementation of the Wave Watch III (WW3) model in the Mediterranean Sea, delivered by INGV (Istituto Nazionale di Geofisica e Vulcanologia), see *Clementi et al. (2017)*. The model is horizontally discretized on a 1/16 (3.75 M in the meridional direction) mesh and hourly output fields are employed.

3. Results

In order to demonstrate the impact of ocean currents on optimal routes, we perform a case study in a marine region at the boundary between the Atlantic Ocean and the Mediterranean Sea. This region comprises the eastern part of the Gulf of Cadiz and most of the Alboran Sea, whose eastern boundary is conventionally set at about 1° W, *Fourcy and Lorvelec* (2012). The ventilation in the Alboran Sea is typically characterized by zonal winds: either westerly winds through Gibraltar or easterlies, *Ardhuin et al.* (2007), *Macías et al.* (2008). Both of them can easily lead to waves exceeding 3 m in significant height over distances of the order of 100 M.
The surface circulation in the Alboran Sea is normally characterized by two main anticyclonic eddies

formed by the surface Atlantic jet entering the Mediterranean Sea. These eddies have a radius of curvature of about 10 M and their magnitude can occasionally exceed 2 kn. The western eddy or WAG is typically centered at about 4°30' W, while the eastern one or EAG is centered at about 3° W. The WAG is the more robust of the two eddies, with the EAG weakening and eventually disappearing during the winter months, *Peliz et al*. (2013).

The vessel considered for the case study is a trawler whose parameters are provided in Tab. II. The drag coefficient C_T of its hull is modeled with an exponent $q=2$ (Sect.2.2), corresponding to a calm water resistance scaling with the fourth power of STW. Both the calm water and the wave added resistances as functions of significant wave height are displayed in Fig.1a. They determine the sustained STW, that is displayed in Fig.1b at both the full and minimum throttle. The Froude Number is given by $STW/\sqrt{(g\ L)}$, with the vessel length at waterline L of Table II and the standard gravitational acceleration g=9.80665 m/s^2.

Table II: Vessel propulsion parameters, principal particulars, and drag coefficient exponent used in this work

P_{max}	Max engine brake power	650 hp
v_{max}	Top speed	10.7 kn
L	Length at waterline	22 m
B	Beam	6 m
T	Draught	2 m
T_R	Natural roll period	5.4 s
q	Exponent in drag coefficient C_T	2

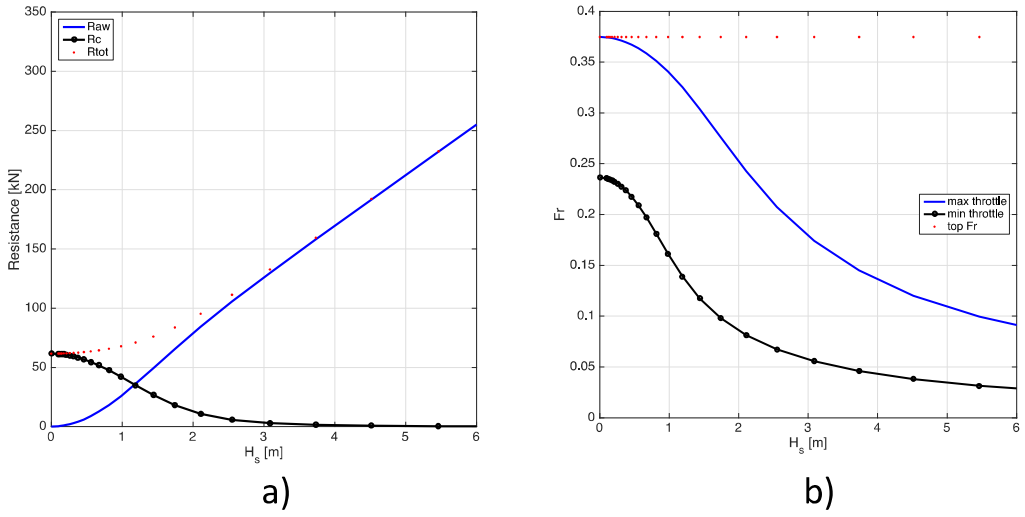

Fig.1: Dynamic properties of a vessel with parameters as in Tab.II. a) Calm water (Rc), wave-added resistance (Raw), and their sum (Rtot). b) Sustained Froude Number at maximum and minimum (=10% maximum) engine throttle. For both panels the independent variable is the significant wave height.

In the first two case studies considered in this work, F1 and F2, the vessel departs west of Gibraltar and reaches a location at the same latitude and about 200 M East, in the Alboran Sea. In the latter two cases, B1 and B2, departure and arrival location are swapped and the departure date is more than one month later.

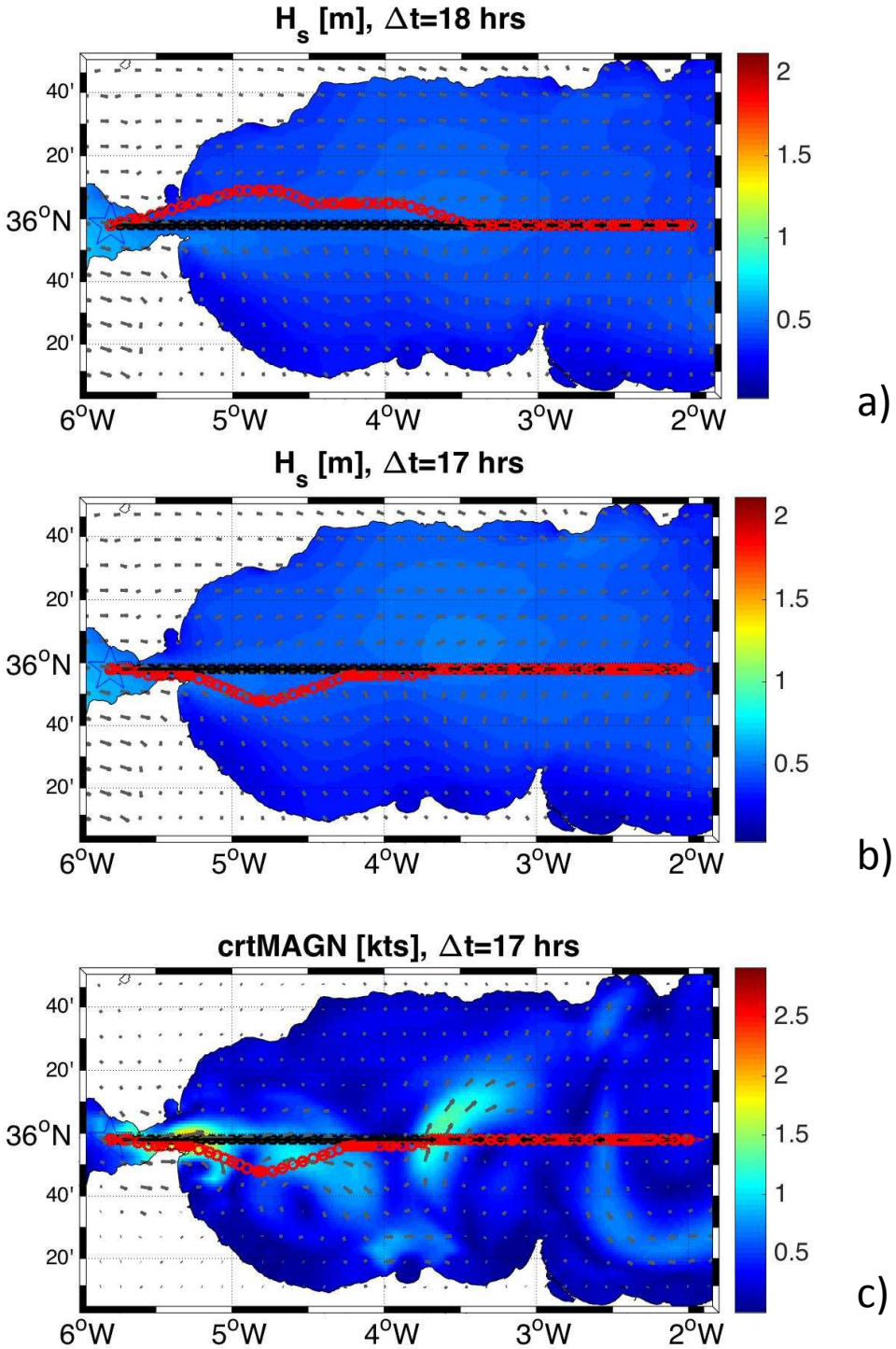

Fig.2: Case studies F1 (no current) and F2 (with current). Geodetic route in black and optimal route in red. The fields in background refer to the time of arrival of the optimal route. a) F1 and wave field; b) F2 and wave field; c) F2 and surface current field. Red arrows in b) and c) denote vessel heading. Route animations available at https://av.tib.eu/media/21737, https://av.tib.eu/media/21738, ~~https://av.tib.eu/media/217439~~ for panel a), b), and c) respectively.

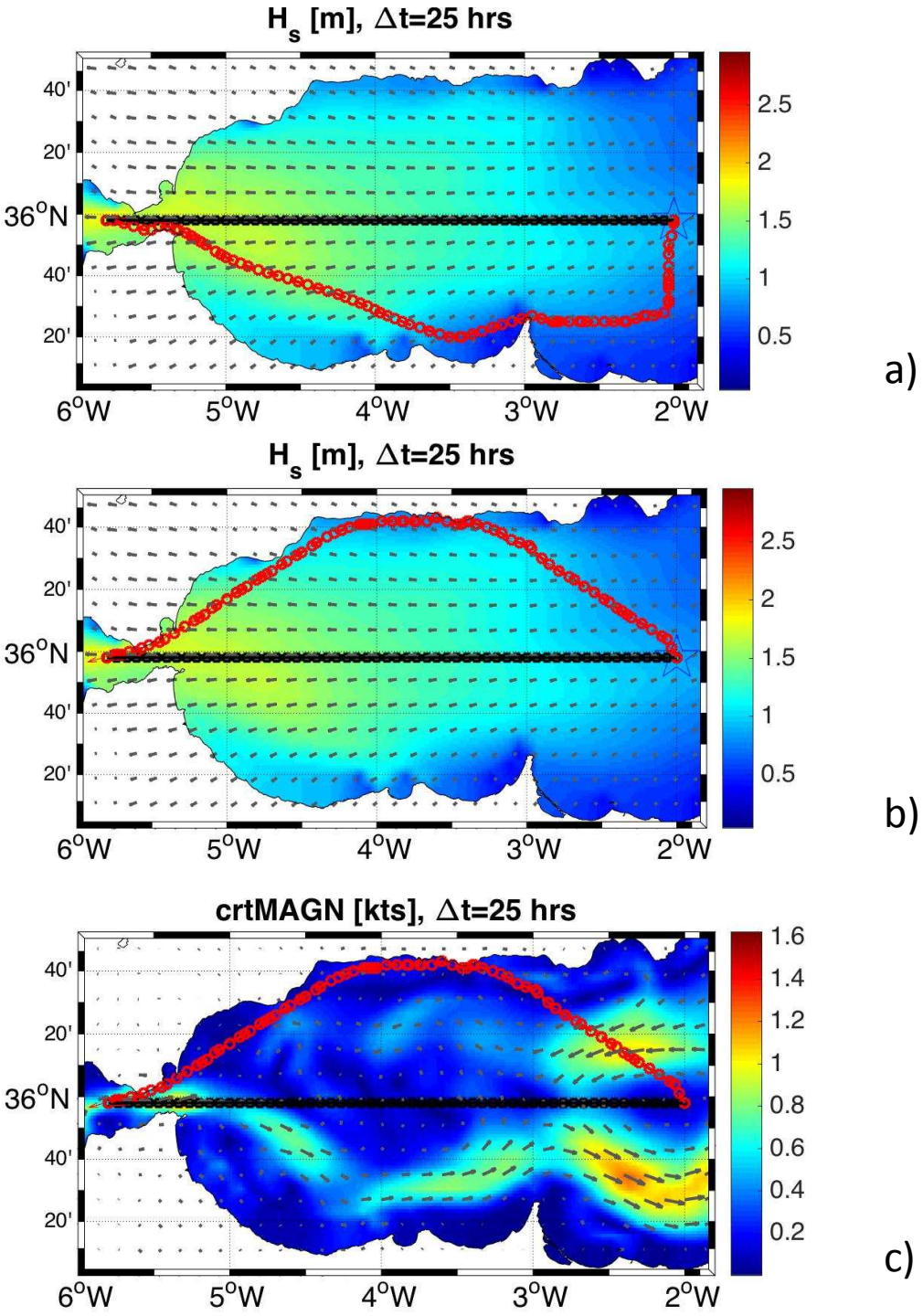

Fig.3: Case studies B1 (no current) and B2 (with current). Geodetic route in black and optimal route in red. The fields in background refer to the time of arrival of the optimal route. a) B1 and wave field; b) B2 and wave field; c) B2 and surface current field. The red arrows in b,c) denote vessel heading. Route animations available at https://av.tib.eu/media/21740, https://av.tib.eu/media/21741, https://av.tib.eu/media/21742 for panel a), b), and c) respectively.

For each case, both a geodetic and an optimal route are computed. The geodetic route (black markers in Fig.2 and Fig.3) is the shortest route keeping into account the coastline and the under keel clearance only. The optimal route (red markers in in Fig.2 and Fig.3) also considers the impact of the environmental fields (Sect.2.4) on STW and SOG and the dynamical constraints for vessel intact stability (Sect 2.2).

The presentation strategy of the case studies is the following: first, the geodetic and the optimal route in presence of waves only are displayed on top of the significant wave height field (panels a in Fig.2 and Fig.3); then both routes in presence of waves and currents are displayed on top of either the significant wave height field (panels b) or the surface current field (panels c). The main computational and dynamical parameters of the routes are summarized in Table III and IV respectively.

Table III: Computational parameters of case study routes. Departure date is on the day following the model analysis date. The total CPU time does not include the time for the graphical rendering of maps and time series. The number of nodes and edges in the graph is respectively 19'271 and 1'468'703 for each case study.

Case study#	Currents considered?	Model analysis date	Depart time	#time -steps	Opt. route CPU time [s]	Total CPU time [s]
F1	No	2016-08-28	21:00 UTC	19	6.9	54.5
F2	Yes			18	7.0	61.9
B1	No	2016-12-28	03:00 UTC	26	8.2	123.6
B2	Yes			26	8.2	138.5

Table IV: Dynamical features of case study routes. Δ is the relative change of metrics (length, duration) of the optimal route with respect to the case with surface currents neglected.

Case study #	Currents considered?	Length [m]			Duration [hh:mm:ss]	
		Geodetic	Optimal	Δ [%]	Optimal	Δ [%]
F1	No	184.9	188.2	0.0	18:00:06	0.0
F2	Yes		188.4	+0.1	17:28:01	-3.0
B1	No		223.0	0.0	25:28:33	0.0
B2	Yes		211.0	-5.4	25:24:30	-0.3

Table V: Route analysis dates and some marine weather features. Departure date is on the day following the model analysis date. For each date departure times at 00:00, 03:00, 06:00, 09:00, 12:00, 15:00, 18:00, 21:00 UTC are considered, which makes the 40 dots per panel of Fig.4

Analysis date	Case study	Prevailing wave direction	WAG?	EAG?
2016-08-28	F1, F2	eastbound	Yes	North-western meander only
2016-10-24	-	East- and then southwestbound	Yes	Yes
2016-12-28	B1, B2	westbound	southern meander only	cyclonic
2017-01-12	-	eastbound	Yes	No
2017-01-25	-	southwestbound	Yes	Yes

In the "wave-only" forward route, F1, the vessel sails with following waves. A northbound diversion (Fig.2a) instrumental in avoiding a condition of surfriding/broaching-to is computed (not shown). In the "wave&current" forward route F2 instead a southbound diversion is observed (Fig.2b,c). This is not surprising, as the algorithm exploits the favorable eastbound jet (more than 2 kn velocity) of the Atlantic current that feeds the WAG. The optimal route is 3% faster than the case not considering currents, Table IV. In this case, the currents allow not just recovering the involuntary speed loss due

to the added resistance in waves, but even achieving a voyage-average speed of 10.8 kn, i.e. nearly 1% higher than the top speed of the vessel in calm waters, Table II.

In the "wave-only" backward route, B1, a westbound route leg follows a sudden southbound diversion (Fig.3a), and this is due to avoidance of both pure loss of stability (not shown) and rough sea (cf. route animation at https://av.tib.eu/media/21740). The algorithm also computes throttle reductions down to 55% brake power (not shown). In the "wave&current" backward route, B2, a large northbound diversion is found (Fig.3b,c). This allows avoiding a SOG penalty in sailing across and then against the southern meander of the WAG and allows exploiting the favorable northern meander of the EAG. The route then continues in the coastal waters of Andalusia where calm seas are encountered, realizing that "route refraction" that was already explained in *Mannarini et al*. (2016b) and aimed to benefitting from to the larger STW in calmer sea. During the crossing of the northern meander of the EAG, the rudder must be set more than 10° starboard of the Course Over Ground (COG, not shown). The B2 route is more than 5% shorter than the B1. However, the maximum SOG along B2 is about 1 kn less than along B1.

4. Conclusions

The ship routing model VISIR has been generalized for accounting for both sea state variables and surface currents. If the vessel course is prescribed, currents affect both the SOG and the rudder angle of the vessel, while the STW is determined by the sea state only (specifically, by the significant wave height).

Case studies in the Alboran Sea are discussed. VISIR attempts to maximize the sailing with currents and minimize navigation against or cross the currents. The duration of the resulting least-time routes can differ in percent range from the ones neglecting the currents and their topology can be dramatically different.

However, the ocean circulation and the sea state obtained from data-assimilative forecasting models show such a variability to rule out not only the use of climatological currents and waves, but also to limit the conclusions drawn from individual time-dependent case studies.

Thus, these numerical results from VISIR should be consolidated through a wider set of routes and vessel types in different regions of the global ocean. Nevertheless, these results already provide first evidence that, at least for not too fast fishing vessels, ocean currents may have a measurable impact on route duration and topology, even in presence of waves.

Acknowledgements

This work has received partial funding from the European Union's Horizon 2020 research and innovation programme under grant agreement No 633211 ("AtlantOS").

References

ALEXANDERSSON, M. (2009), *A study of methods to predict added resistance in waves*, Master thesis, KNH Centre for Naval Architecture, Stockholm
www.knh.se/polopoly_fs/1.151543!/Menu/general/column-content/attachment/Alexandersson.pdf

ARDHUIN, F.; BERTOTTI, L.; BIDLOT, J.R.; CAVALERI, L.; FILIPETTO, V.; LEFEVRE, J.M.; WITTMANN, P. (2007), *Comparison of wind and wave measurements and models in the Western Mediterranean Sea,* Ocean Engineering 34(3), pp.526-541

BAZARI, Z.; LONGVA, T. (2011), *Assessment of IMO mandated energy efficiency measures for international shipping*, International Maritime Organization, http://www.imo.org/

BERTSEKAS, D.P. (1998), *Network Optimization: Continuous and Discrete Models,* Athena Scientific, http://web.mit.edu/dimitrib/www/netbook_Full_Book.pdf

BREIVIK, Ø.; ALLEN, A.A. (2008), *An operational search and rescue model for the Norwegian Sea and the North Sea*, J. Marine Systems 69, pp.99-113, https://arxiv.org/pdf/1111.1102.pdf
CHANG, Y.C.; TSENG, R.S.; CHEN, G.Y.; CHU, P.C.; SHEN, Y.T. (2013), *Ship routing utilizing strong ocean currents*, J. Navigation 66, pp.825-835, www.dtic.mil/dtic/tr/fulltext/u2/a587298.pdf

CHEN, H.H. (1978), *A dynamic program for minimum cost ship routing under uncertainty*, Ph.D. thesis, Massachusetts Institute of Technology

CLEMENTI, E.; ODDO, P.; DRUDI, M.; PINARDI, N.; KORRES, G.; GRANDI, A. (2017), *Coupling hydrodynamic and wave models: first step and sensitivity experiments in the Mediterranean Sea*, Ocean Dynamics

FOURCY, D.; LORVELEC, O. (2012), *A new digital map of limits of oceans and seas consistent with high-resolution global shorelines,* J. Coastal Research 29(2), pp.471-477

GERRITSMA, J.; BEUKELMAN, W. (1972), *Analysis of the resistance increase in waves of a fast cargo ship,* International Shipbuilding Progress 19, pp.285-293

LO, H.K.; McCORD, M.R. (1995), *Routing through dynamic ocean currents: General heuristics and empirical results in the Gulf stream region*, Transportation Research Part B: Methodological 29, pp.109-124

LO, H.K.; McCORD, M.R. (1998), *Adaptive ship routing through stochastic ocean currents: General formulations and empirical results*, Transportation Research Part A: Policy and Practice 32, pp.547-561

LOLLA, T.; HALEY, P.J.; LERMUSIAUX, P.F. (2014), *Time-optimal path planning in dynamic flows using level set equations: realistic applications*, Ocean Dynamics 64, pp.1399-1417

MACÍAS, D.; BRUNO, M.; ECHEVARRÍA, F.; VÁZQUEZ, A.; GARCIA, C.M. (2008), *Meteorologically-induced mesoscale variability of the North-western Alboran Sea (southern Spain) and related biological patterns*, Estuarine, Coastal and Shelf Science 78(2), pp.250-266

MANNARINI, G. (2015a), *The twofold aspect of climate change on navigation: the search for new maritime routes and the challenge of reducing the carbon footprint of ships*, Tech. Rep. RP0252, CMCC, http://www.cmcc.it/wp-content/uploads/2015/03/rp0252-opa-03-2015.pdf

MANNARINI, G.; LECCI, R.; COPPINI, G. (2015b), *Introducing sailboats into ship routing system VISIR,* 6th Int. Conf. Information, Intelligence, Systems and Applications, pp.1-6

MANNARINI, G.; PINARDI, N.; COPPINI, G. (2016a), *VISIR: A free and open-source model for ship route optimization,* COMPIT Conf., Lecce, http://data.hiper-conf.info/compit2016_lecce.pdf

MANNARINI, G.; PINARDI, N.; COPPINI, G.; ODDO, P.; IAFRATI, A. (2016b), *VISIR-I: small vessels – least-time nautical routes using wave forecasts*, Geoscientific Model Development 9, pp.1597-1625, http://www.geosci-model-dev.net/9/1597/2016/gmd-9-1597-2016.pdf

MANNARINI, G.; TURRISI, G.; D'ANCA, A.; SCALAS, M.; PINARDI, N.; COPPINI, G.; PALERMO, F.; CARLUCCIO, I.; SCURO, M.; CRET`ı, S.; LECCI, R.; NASSISI, P.; TEDESCO, L.

(2016c), *VISIR: technological infrastructure of an operational service for safe and efficient navigation in the Mediterranean Sea,* Natural Hazards and Earth System Sciences 16(8), pp.1791-1806, http://www.nat-hazards-earth-syst-sci.net/16/1791/2016/nhess-16-1791-2016.pdf

PELIZ, A.; BOUTOV, D.; CARDOSO, R.M.; DELGADO, J; SOARES, P.M. (2013), *The Gulf of Cadiz–Alboran Sea sub-basin: Model setup, exchange and seasonal variability,* Ocean Modelling 61, pp.49-67

SUBRAMANI, D.N.; LERMUSIAUX, P.F. (2016), *Energy-optimal path planning by stochastic dynamically orthogonal level-set optimization*, Ocean Modeling 100, pp.55-57

TONANI, M.; ODDO, P.; KORRES, G.; CLEMENTI, E.; DOBRICIC, S.; DRUDI, M.; PISTOIA, J.; GUARNIERI, A.; ROMANIELLO, V.; GIRARDI, G.; GRANDI, A.; BONADUCE, A.; PINARDI, N. (2014), *The Mediterranean Forecasting System: recent developments*, EGU General Assembly Conference Abstracts 16, p.16899

TONANI, M.; BALMASEDA, M.; BERTINO, L.; BLOCKLEY, E.; BRASSINGTON, G.; DAVIDSON, F.; DRILLET, Y.; HOGAN, P.; KURAGANO, T.; LEE, T.; MEHRAK, A.; PARA-NATHARAL, F.; TANAJURAM, C.; WANG, H. (2015), *Status and future of global and regional ocean prediction systems*, J. Operational Oceanography 8, s201–s220

ZOPPOLI, R. (1972), *Minimum-time routing as an N-stage decision process*, J. Applied Met. 11, pp.429-435, http://journals.ametsoc.org/doi/pdf/10.1175/1520-0450(1972)011%3C0429:MTRAAS%3E2.0.CO%3B2